Nuclear Spallation and Neutron Capture Induced by Ponderomotive Wave Forcing

Rickard Lundin and Hans Lidgren

IRF Scientific Report 305

October 2015

ISSN 0284-1703

Institutet för rymdfysik

Swedish Institute of Space Physics

Kiruna, Sweden

Nuclear Spallation and Neutron Capture Induced by Ponderomotive Wave Forcing

Rickard Lundin and Hans Lidgren

IRF Scientific Report 305

October 2015

Institutet för rymdfysik

Swedish Institute of Space Physics

Kiruna, Sweden

IRF Scientific Report 305
ISSN 0284-1703

Swedish Institute of Space Physics
Box 812
SE-981 28 Kiruna
SWEDEN
www.irf.se

Nuclear Spallation and Neutron Capture induced by Ponderomotive Wave Forcing

[1]Rickard Lundin and [2]Hans Lidgren
[1]*Swedish Institute of Space Physics, Box 812, 981 28 Kiruna, Sweden*
[2]*Le Mirabeau, 2 ave des Citronniers, MC 98000, Monaco*
(Dated: 12 October 12, 2015)

We demonstrate that nuclear energy may be derived from a two-stage process: 1) thermal neutron spallation induced by resonant Ponderomotive wave forcing, and 2) isotopic transmutations by thermal neutron capture of heavier elements. While the former (spallation) consumes energy, the latter (neutron capture) produces energy, the combined process leading to a net energy output. The combined process is here labeled Resonant Isotopic Transmutation of Nuclides, RIToN.

The main empowering process producing neutrons, as well as enabling centralized attraction, is the ponderomotive Gradient/Miller (G/M) force. The G/M force has three unique properties, it: (1) is induced by electromagnetic wave penetration into matter. (2) Has a bipolar singularity at wave resonance, attractive below-, and repulsive above resonance. (3) Is charge neutral, i.e. positive ions and electrons are jointly forced in the same direction. Fast neutron spallation, an important criterion for RIToN, requires efficient wave acceleration, i.e. waves at frequencies at/near particle resonance

Two suitable elements are considered for neutron spallation in the RIToN process, deuterium and lithium. From the process ^{2}H —> H and ^{7}Li —> ^{6}Li, and their differences in binding energy, neutrons may be derived at the expense of an energy input 2.25 MeV and 7.25 MeV respectively. The subsequent capture of free neutrons is besides favoring isotopes with high neutron capture cross-sections, also highly dependent on the magnitude of the G/M force. A number of isotopes capable of releasing excess energy, and having reasonably high neutron capture cross sections are feasible, such as ^{58}Ni —> ^{62}Ni, and ^{40}Ca —> ^{42}Ca. Furthermore, the excess energy from thermal neutron capture leads to a chain-reaction; enhanced spallation, further enhanced energy production etc, leading to an almost self-sustained process.

The Gradient/Miller force and Abraham force [1] exemplifies ponderomotive forcing by electromagnetic waves. The basis for ponderomotive forcing is that electromagnetic waves transfer energy and momentum to matter. Intuitively, wave-induced ponderomotive forces are expected to be repulsive, i.e. the "heaviness" (in Latin *ponderos*) of waves provides a transfer of energy and momentum in the direction of wave propagation. However, as discussed in a review [1], ponderomotive forces are multifaceted, with consequences that may contradict intuition. An example of that is magnetic moment pumping, MMP, a ponderomotive force in magnetized plasmas with diverging magnetic fields. The MMP force [1, 2] is always in the direction of the magnetic field divergence - regardless of wave propagation direction and wave frequency. The MMP force exemplifies that the term "heaviness" can be a misleading.

The Gradient/Miller force [1, 3] is a more conspicuous exception to the intuitive concept of "heaviness" of waves. The direction of the Gradient force in plasmas critically depends on the local resonance frequency, e.g. the ion gyro frequency, Ω. For Alfvén waves in magnetized plasma, the Gradient force is repulsive at frequencies above-, and attractive at frequencies below Ω.

A number of studies show that wave-induced ponderomotive forcing may be a useful way to describe wave forcing of space plasma, such as the transfer of energy and momentum by Alfvén waves, and ion cyclotron waves [4, 5, 6, 7]. Following the proposal by Alfvén [8] on the existence of magnetohydrodynamic (MHD) waves, attempts were made to prove the existence of MHD waves in laboratory. A series of experiments carried out at the Royal Institute of Technology in Stockholm proved the existence of the transverse Alfvén mode in magnetized mercury [9, 10] and magnetized liquid sodium [11]. While Alfvén waves is a major issue in contemporary space and astrophysical plasma studies, only a few papers on MHD wave propagation in magnetized solid-state plasmas have been published after the proof of existence in the 1950ies, [12, 13 14]. Mass-transport in solid-state plasmas observed in connection with microwave radiation [15], was consistent with ponderomotive the force expression introduced by Miller [7]. Other theories and laboratory results on ponderomotive forcing in plasmas [16, 17, 18, 19, 20], in particular those related with resonance absorption [19, 20] are relevant in context with this study.

The abovementioned reports demonstrate that conducting solid bodies may be treated as plasma (solid-state plasma). The concept of ponderomotive forcing, specifically the Gradient force may therefore be applied to matter at a variety of states - solid, fluid, gas, and plasma. For two reasons, we have chosen the Alfvén wave analogy in deriving the Gradient force. First, Alfvén waves have been observed in plasmas at all states, plasma, gaseous-, liquid-, and solid-state. Secondly, Gradient forcing by Alfvén waves have a frequency independent response below resonance.

Ponderomotive wave forcing of plasmas and neutrals

Ponderomotive forces are time-averaged nonlinear forces acting on a media in the presence of oscillating electro-magnetic fields. The concept is used to facilitate the

solution of dynamical problems. By averaging over the period of oscillations, dynamical problems are more easily solved, compared to that using the simple Lorentz force.

All ponderomotive forces are characterized by a nonlinear (quadratic) dependence on the amplitude of the oscillating wave electric field. They can be divided in two categories, distinguished by their difference in *temporal and spatial derivatives* in the force expression.

Of the five potential ponderomotive effects [3], the Gradient force and the Abraham force are considered most powerful in a weakly magnetized, or magnetic gradient-free environment. However, depending on the heating method (e.g. induction) effects of the magnetic gradient force (MMP) is also viable. Moreover the Barlow force [1], induced by gas particle collisions may influence the dynamics of the system.

For reasons already discussed, Alfvén (magneto-hydrodynamic) waves are a useful plasma fluid wave-mode. Since the ion mass is typically >1800 times higher than the electron mass, the electron mass can be neglected. The mass density and the corresponding forcing upon the plasma is therefore determined by the ion mass, m. Alfvén waves propagate along magnetic field lines (**k**=(0,0,k)) and have linear polarization

The following expression applies for the longitudinal (along z) Gradient force (in cgs units) governed by Alfvén waves in a fluid [1].

$$F_Z = -\frac{e^2}{4m\left(\omega^2 - \Omega^2\right)}\frac{\partial E^2}{\partial z} \qquad (1)$$

Where $\delta E^2/\delta z$, i.e. the spatial gradient of the wave electric field determines the magnitude of the force, and Ω is the ion cyclotron (resonance) frequency. Notice that the expression has a singularity at $\omega = \Omega$, the Gradient force being attractive for $\omega < \Omega$, and repulsive for $\omega > \Omega$. The implication of this is that low-frequency Alfvén waves ($\omega < \Omega$,) attract charged particles towards the wave source, while high-frequency Alfvén waves repel particles.

Similarly, the longitudinal Abraham force (2) by Alfvén waves [1] is given by:

$$F_z = \pm\frac{mc^2}{2c_A B^2}\frac{\partial E^2}{\partial t} = \pm\frac{c\sqrt{\mu_0\rho}}{2eB_z\Omega^2}\frac{\partial E^2}{\partial t} \qquad (2)$$

Where the +(-) sign corresponds to the wave propagation parallel (antiparallel) with the direction of the magnetic field B, $\delta E^2/\delta t$ is the temporal variation of the wave electric field determining the magnitude of the force, c_A is the Alfvén velocity, and ρ is the mass density of the fluid. The Abraham force may be significant for fast changes of E ($\delta E^2/\delta t$) and weak magnetic fields (low cyclotron resonance frequencies). However, as will be discussed later, low resonance frequencies give low neutron production rates. The merit of the Abraham force may instead be to promote heating by the fast directional electromagnetic field changes, and to maintain longitudinal focusing in the reactor. Nevertheless, the quantitative analysis on ponderomotive forcing will be focused on the Gradient force. Figure 1 gives a diagrammatic representation of the Gradient force and the Abraham force.

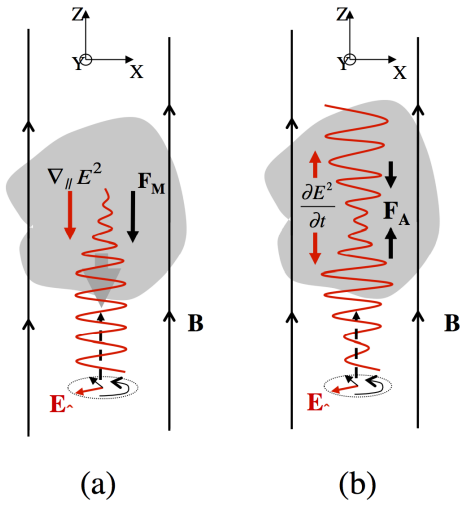

(a) (b)

Fig. 1 Summary diagram of two ponderomotive forces in plasma, expected to play a role in the RIToN process, (a) the gradient/Miller force, and (b) the time dependent electric field Abraham force (after [1], Fig 6).

Notice that the Gradient force (expression 1) does not depend on the sign of charge (e^2). *The Gradient force is charge-neutral, i.e. it applies to neutral matter as well.* Since neutral matter on an atomic and nuclear level constitute charges, one may therefore consider atomic oscillations (e.g. Brownian motions) and interatomic vibrations as "fundamental frequencies". The electric field term of e/m waves should therefore affect solids in a similar way as plasma bound by a strong magnetic field. In what follows, the Gradient force on matter in the neutral state (gas, fluid, solid) will be described.

The fact that electromagnetic waves in plasma may lead to attraction is not obvious. However, this can be demonstrated by using MHD theory. MHD waves are a class of waves in fluids where plasma and magnetic field display a mutual oscillation, the plasma considered "frozen" into the magnetic field. In a spatially unidirectional magnetic field the plasma resonance frequency, rather than the direction of wave propagation (+z-direction), determines the direction of the force. However, in the low-frequency case, $\omega^2 << \Omega^2$, using $\Omega = eB/mc$ we obtain from expression (1):

$$F_Z = \frac{mc^2}{4B}\frac{\partial E^2}{\partial z} \qquad (3)$$

This implies that the force is constant and independent of wave frequency in a homogeneous medium (B = constant) at very low frequencies, the force being proportional to the gradient and magnitude of the EM-wave intensity ($\partial E^2/\partial z$). Because the wave intensity is decreasing during interaction (exerting force on matter) the force F_z is directed opposite to the wave propagation direction.

The concept of MHD waves stems from the fluid description of plasmas. MHD waves are governed by the magnetic tension in magnetized plasma - the stronger the magnetic tension, the weaker the wave group velocity and Gradient force. In a similar way, MHD waves in solid-state plasma are governed by their dielectric properties and interatomic tension. While the local resonance frequency in gaseous magnetized plasma is determined by the ion gyro frequency, the local resonance frequency in neutral solids and neutral gases, comprising atoms is less obvious. However, as already noted, the Gradient force is charge-neutral, implying that the force on the positive (protons) and negative (electrons) charged particles goes in the same direction. The analogy with MHD waves in plasma is useful, because ideal MHD implies no particle transport *per se* in matter. However, matter will be subject to forcing by the intrusion, and damping of wave energy, the force determined by a spatial gradient of the wave electric field.

For un-magnetized neutrals the analogy implies that wave energy can penetrate, the Gradient force working on atomic protons and electrons collectively. At very low frequencies (expression 3) the force is weakly attractive, regardless of atomic structure or mass. However, approaching resonance frequency (expression 1) the Gradient force increases non-linearly. Resonance frequencies in plasma physics are related to the intrinsic fluid properties, such as plasma density, particle mass/inertia, and the magnetic field. The same should apply for solid state, except that mechanical and interatomic Van de Wahl binding forces are involved as well. An investigation of typical plasma and neutral resonances will be considered, the reason being that both may apply for the e/m wave Gradient force.

Under the assumption that the e/m waves irradiating the neutral fluid/body are linearly polarized, the Gradient force exerted on individual particles/atoms of mass m_a by a radiation electric field E becomes:

$$F_z = -\frac{e^2}{4m_a\left(\omega^2 - \Omega_a^2\right)}\frac{\partial E^2}{\partial z} \qquad (4)$$

The theoretical Gradient force versus frequency in expression (4) resembles that of expression (2), except that we have introduced the hitherto undefined resonance frequency, Ω_a. Noting, again that ponderomotive/gradient forcing affect plasma as well as matter in the neutral state [9, 10, 11, 21, 22], it is useful to consider the analogy between the magnetic (Lorenz) force in plasmas and the interatomic (Van de Wahl) force in solids, fuels, and gasses. The forces are motion-related, i.e. governed by the particle velocities/energies. Both forces are effectively zero (force balanced) when particles/atoms at rest. Only when the ions have finite energies/velocities do the Lorenz force operate, ions describing cycloid motions at cyclotron frequencies Ω. Similarly, inter-atomic resonances of neutral matter at a frequency Ω_a require finite atomic (Brownian) motional velocities. However, as noted in the forth-coming sections, the enabling part in the RIToN process, neutron spallation, is assumed to be in the plasma state. On the other hand, neutron capture is considered to take place in neutral matter.

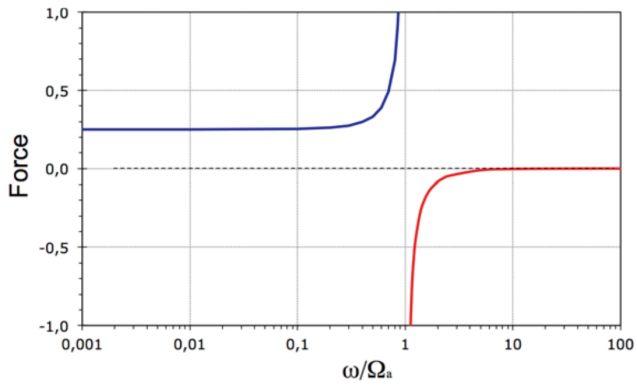

Fig. 2 Alfvén wave Gradient force versus normalized frequency for unit material constant ($e^2/4m_a=1$), and $\partial E^2/\partial z=0.25$ (expression 4). Blue curves marks attractive force, red curve repulsive force.

Fig. 2 describes the Gradient force versus frequency. Notice that the Gradient force is independent of wave frequency for $\omega << \Omega$ and attractive over the entire frequency range below resonance. Above resonance, the force is repulsive. At frequencies well below resonance, $\omega << \Omega$, the following expression for the Gradient force applies [21]:

$$F_Z = \frac{a^2e^2}{4mc^2}\frac{\partial E^2}{\partial z} = \xi_A(a,m)\frac{\partial E^2}{\partial z} \qquad (5)$$

The force depends on a material constant, $\xi_A(a,m)$, where A indicates the atomic mass number, and δE the spatial gradient (damping) of the wave electric field propagating into matter. Wave attraction is determined by the spatial gradient of E, i.e. $\delta E^2/\delta z$, where δz is the differential interaction length. The material constant $\xi_A(a,m)$, the gradient $\delta E^2/\delta z$, and the transverse wave electric field E, now determines the Gradient force exerted on matter. Notice that a, representing the atomic separation distance in matter (solid, fluid, gas), defines the half wavelength/ground frequency of mutual interatomic oscillations, in analogy with the motion of ions and electrons in a magnetic field. Furthermore, because fluid theory is applicable for plasma as well as neutrals, especially if the plasma is non-magnetized, we may use acoustic wave theory in e.g solids, neutral gas, and plasmas to determine their specific resonant conditions, as discussed in the next section.

Fig. 3 summarizes two aspects of the low-frequency Gradient force attraction, the first (Fig. 3a) demonstrating the experimental findings from the Cavendish experiment [21, 22], the second (Fig. 3b) describing fundamentals of this report, centralized Gradient force attraction of matter towards a radiating hot core.

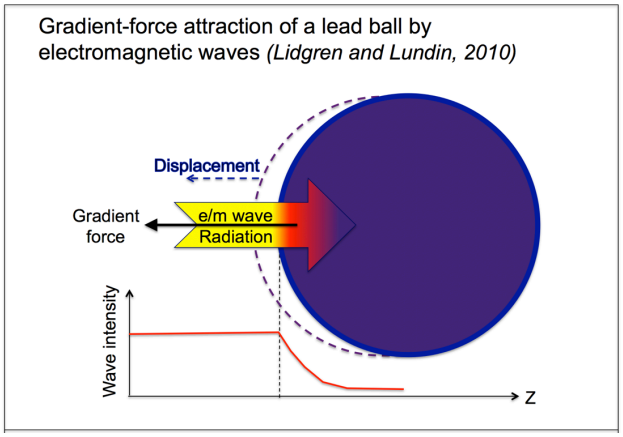

Fig. 3a Diagrammatic representation of electromagnetic wave attraction observed in a Cavendish experiment [22].

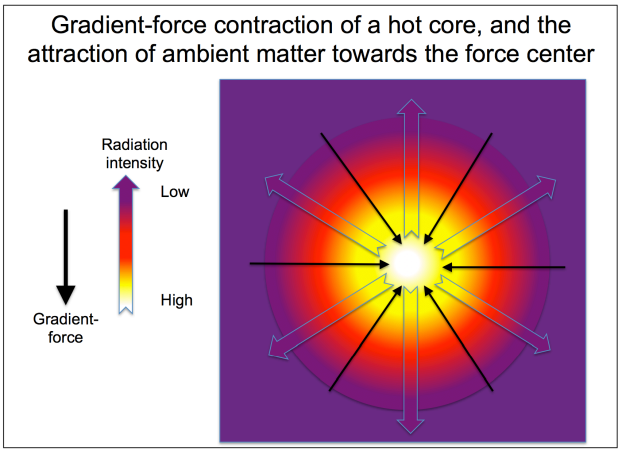

Fig 3b. Diagrammatic illustration of the reactor concept based on centralized Gradient force attraction of matter.

Ion resonance acceleration and neutron spallation by Ponderomotive Forcing

An overview of the elements involved, and a summary of the isotope changes and boundary conditions (binding energy, ΔE, thermal neutron capture cross section, etc) to maintain the RIToN process, is given in Tables 1 and 2, where Table 1 display two of the critical elements required for the RIToN process, i.e. the isotopes and the corresponding isotope shifts that leads to neutron spallation (^{7}Li + energy —> ^{6}Li + 1 n) and neutron capture (^{58}Ni + x·n —>$^{58+x}$Ni + energy). In what follows the abovementioned theoretical background is used to determine the combined ion resonance acceleration and central target attraction by ponderomotive/Gradient forcing of a fuel consisting of lithium - nickel, or deuterium - nickel. In Table 2 a comparison is made between the spallation of ^{7}Li and ^{2}H, demonstrating that the thermal neutron yield per MeV is 3.3 times higher for ^{2}H spallation. However, the abovementioned yields are theoretical based on the external power input as igniter for the RIToN process. Eventually, internally driven excess power becomes the main driver for neutron spallation. Notice also from Table 2 that neutron capture of ^{63}Ni , and ^{65}Ni is possible. Via β^{-}-decay ^{63}Ni , and ^{65}Ni goes to the stable elements ^{63}Cu and ^{65}Cu, clearly element shifts. However, these element shifts do not involve proton fusion; they result from a loss of charge via β^{-}-decay. The charge-shift for unstable isotopes may also go the other direction, via β^{+}. Element shift is a possible consequence of neutron capture via an unstable isotope.

Based on the expressions 1-5, the Gradient forcing of plasmas as well as neutrals may be considered. However, by virtue of a low boiling point of lithium (1340° C), and in particular deuterium, lithium and deuterium can easily be transferred to the plasma state. This means that we may apply Gradient force theory of plasmas (lithium and deuterium ions). On the other hand, the high melting/boiling point of nickel (1455/2913 °C) implies that it may remain in solid or liquid form up to high temperatures. Notice that the above temperatures and states relates to normal temperature and pressure (NTP). The above boiling points increases with pressure, implying that a pressurized reactor may operate at temperatures well above the boiling point for nickel at NTP. Conversely, a low-pressure reactor environment enables operation at low temperatures.

Nickel embodies the internal power/heat source via neutron capture, while spallation is a cooling factor for lithium and deuterium. Nickel is therefore the main attractor of matter within the reactor confinement.

Most reactor concepts [e.g. 23, 24] are using metallic cylinders containing small amounts (a few grams) of fuel. The reactor fuel mostly considered is lithium and nickel, but deuterium - nickel fuel has also been used. A fuelled metallic tube constitutes the reactor core. To conserve the heat production in the core, and to moderate the neutron flux, the reactor core is embedded in a layer of aluminum-oxide ceramics. Induction heating by one or several coils wrapped around, or embedded in the insulating ceramics, is used to initiate the internal power generation process.

The process, as we conceive it, requires acceleration of ^{7}Li^{+} or ^{2}H^{+} up to spallation energies at rates exceeding ≈10^{14}/s, corresponding to neutron production rates ≈10^{13}/s (assuming 10% efficiency), the inductive power must entail high frequency waves. If not (just heating) the process may at best provide a gain close to nominal values (≈1.4, Table 2).

In some experiments [e.g. 23, 24], square wave induction heating is used, noting that square waves generate broadband waves extending up to high frequencies. The gaseous part of the fuel subjected to square-wave induction may then enter a non-thermal turbulent state, whereby the particle velocity distribution goes from an exponential (thermal) to a power-law (non-thermal) distribution. The latter enhances the contribution and power of high-frequency waves, a criterion enabling enhanced spallation rates. The exterior design controlling the radiated power output, should also affect the spallation processes.

Resonance is the criterion for reaching high neutron production rates, because the Gradient force increases

nonlinearly towards resonance. Enhanced wave forcing close to resonance enables faster acceleration and correspondingly faster spallation rates. Resonance is governed by the physical properties, such as density, pressure, temperature, and state (neutral, ionized) of matter in the reactor cavity. Hence, an adequate reactor control requires knowledge of the specific resonance criteria.

Because the Gradient force is proportional to the wave power (expression 4, 5), geometrical focusing of radiation (onto the fuel) also amplifies the spallation-efficiency. Depending on the geometry, geometrical focusing of the induced power will amplify the Gradient force by a factor κ, leading to a corresponding increase of the Gradient force and the associated neutron production as described in Fig. 4, noting that the force here is derived for wavelengths well below resonance.

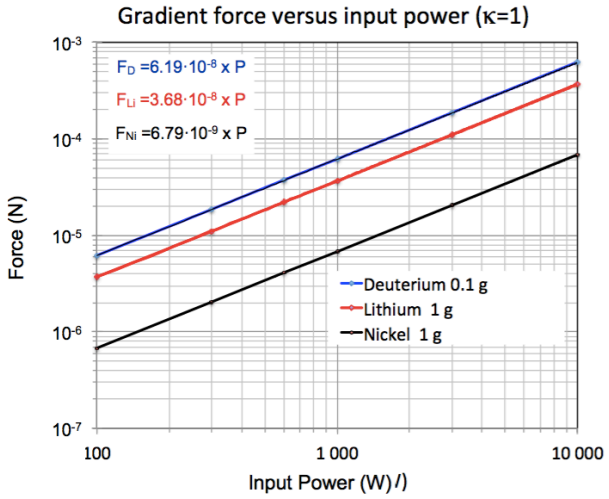

Fig. 4 Gradient force for deuterium (0.1 g), lithium (1 g), and nickel (1 g) versus induced power in a model reactor without power focussing (κ=1) for frequencies well below resonance (expression 5). Notice that the above force curves depend on mass, i.e. the number of atoms affected by the gradient force.

Heating, evaporation and ionization of deuterium and lithium may lead to neutron spallation in the reactor by virtue of a high core temperature, but without wave turbulence/resonance the production rate should be low. On the other hand, combining induction heating with high frequency waves, enhanced spallation rates may be achieved at modest temperatures. A comparison of Figs 2 and 5 demonstrates that the force may be orders of magnitudes higher near resonance. Considering the power of electromagnetic wave forcing of charged particles, in particular in an environment where the ionization rate of the gas may exceed 10^{-2}, electromagnetic wave forcing will be the dominant forcing term for the neutrals as well. It is therefore reasonable to treat the neutron spallation as a process governed by plasma resonances.

Thermal Neutron capture and Isotope Transmutations.

The RIToN process involves two aspects of isotope transmutation, thermal neutron spallation and thermal neutron capture, the former leading to lower-, the latter to higher isotope mass. The mass difference between the two represents the energy gain/loss. The process requires a thermal neutron source and an element with high thermal neutron capture cross-section such as nickel. Maintaining a stable and controlled power output over time requires a mix of "spallation nucleons" (e.g. ^{7}Li) and high-yield thermal neutron capture nucleons (e.g. ^{58}Ni or ^{40}Ca). Neutron-capture starts for stable isotopes with lowest mass (e.g. ^{58}Ni), neutron capture gradually forming isotopes of higher mass (e.g. ^{58}Ni —> ^{62}Ni). Transmutations to unstable isotopes may, if short-lived, lead to element transitions via β-decay, and via neutron capture and another β-decay back to the "original" element. Nevertheless, such charge-exchange transmutations do not alter the isotope transition concept.

To enhance the power from neutron capture, faster neutron spallation rates are required. The latter can be achieved by enhancing the total input power. Besides enhancing the net power output, the latter may also provide a moderate enhancement of the net power Gain from enhanced wave turbulence. However, the most effective power gain is achieved for a tailored wave power input near resonance.

The theoretical ratio between thermal neutron spallation and e.g. Ni^{58} —> Ni^{62} neutron capture varies between ≈1.34 (^{7}Li), and ≈4.32 (^{2}H). Therefore, a process entirely driven by input power thermal neutron spallation would only achieve the abovementioned gains. On the other hand, neutron spallation and neutron capture are mutually beneficial, i.e. internally produced excess power from neutron capture may induce further neutron production. The intrinsic driven excess power may raise the power gain by up to an order of magnitude, compared to the directly driven process.

Simulation of neutron spallation and neutron capture

Figure 2 illustrates that resonance takes place in a very narrow frequency band. A number of resonance conditions are feasible; all depending on the wave modes related with the states of matter – solid, fluid, gas, dusty-plasma, plasma. Considering that the gradient force is charge neutral, i.e. going in the same direction regardless of charge, widens the options to construct a gradient force reactor.

The E-Cat reactor by Rossi and coworkers [23, 24] have demonstrated that a reactor producing at least 3 to 4 times higher output power than input power is feasible. Some characteristics of the E-Cat reactor will be discussed in the next section. For the moment we note that the process responsible for the power output from E-Cat demonstrates quite clearly that it must be due to a nuclear process, a process resembling the one described in this article, RIToN.

Central for the process is to maintain temperature "inertia" and wave resonance, the latter requiring production of waves up to resonance frequencies. A number of resonance frequencies are feasible. The magnitude of the integrated Gradient force onto the fuel

target depends on the state of the element, the frequency (ω), power of the radiation input (P_i), and the geometrical amplification factor (κ) with which the external power (e.g. from an induction coil) is focused on the target. From expression (4, and 5) we derive the following net integrated force:

$$F = -\int F_Z \, dz = -\xi_A \kappa \frac{P_i(\omega)}{\left(\omega^2 - \Omega_a^2\right)} \quad \text{(N)} \qquad (6)$$

Where ξ_A is a material constants derived for lithium is $\xi_{Li}=3.68\cdot10^{-8}$ (N/W), deuterium $\xi_D=6.19\cdot10^{-8}$ (N/W), and nickel $\xi_{Ni}=6.79\cdot10^{-9}$ (N/W). Notice that the force versus power values for deuterium, lithium and nickel in Fig 4 corresponds to $\xi_A\kappa$, i.e. they represent model reactor values. Furthermore, the above values are based on two different fuel mixes in the model reactor; for spallation isotopes 1 g lithium, or 0.1 g deuterium. Regarding neutron capture, 1 g nickel is used in both cases. The ten times higher lithium mass compared to deuterium gives about three times more lithium atoms, i.e. theoretically about three times higher total number of spallated neutrons. However, considering that the deuterium-nickel process is about three times more efficient compared to the lithium-nickel process (Table 2), a ten times higher lithium mass is a reasonable ratio for equal energy production.

Figs. 5a and 5b display the force response versus normalized (to the resonance) frequency for lithium, deuterium, and nickel, Fig. 5a representing the gradient forces per unit power and κ=1, Fig. 5b the force using 800 W input power geometrically focused onto the fuel by a factor κ=5.3 (model reactor). Depending on boundary conditions such as the reactor chamber volume, the content, mix, and state of the fuel, interior and exterior chamber temperature etc, a number of options exist.

We will exemplify the process with two types of resonances relevant to matter in the plasma state, using (1) An ion acoustic resonance of the corresponding gas/plasma ($a=1.1\cdot10^{-9}$ m, $f=7.9\cdot10^{13}$ Hz), and (2) An ion acoustic resonance of a Deuterium gas/plasma (10%), ($a=6.1\cdot10^{-9}$ m, $f=1.3\cdot10^{13}$ Hz). The resonantly forced (F) ion acceleration up to spallation energy (E) may be described by the expression $E\approx F\cdot a\cdot f$ [J]. The total energy required for the spallation of one neutron from e.g. ^{7}Li, 7.25 MeV, corresponds to $1.16\cdot10^{-12}$ J. To produce 10^{14} neutrons/s, close to the minimum rate required to "trigger" the RIToN process, means that an external radiation input power (P_i) producing at least 116 J/s (W) is required. Furthermore, that power source must contain frequencies close to resonance (Fig. 5), operating at higher power (>400 W) to obtain a force >0.01 N. The frequency-dependent neutron production rate, $R(\omega)$, may now be described by the expression:

$$R(\omega) = 2\pi \frac{\eta}{W_S} F(\omega)\cdot a\cdot\omega \qquad (neutrons/s) \qquad (7)$$

Where W_s is the spallation energy, η is an efficiency factor assumed to be greater than 0.1, and ω is the wave angular frequency. Theoretically, there is a linear relation between the radiation input power and the Gradient force well below resonance, meaning that the neutron production rate is proportional to the electromagnetic power applied to the gas/plasma of ^{7}Li or ^{2}H. The power versus neutron production rate relation is displayed in Fig. 6, under the assumption of a neutron production efficiency η =0.5.

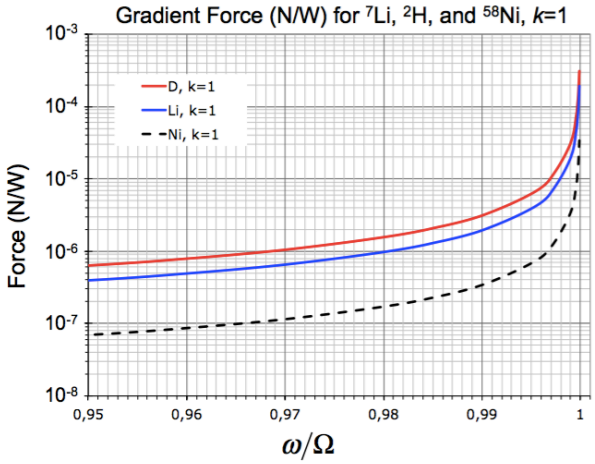

Fig. 5a Force per unit input power and unit geometrical focusing, demonstrating the non-linear increase of the gradient force near resonance.

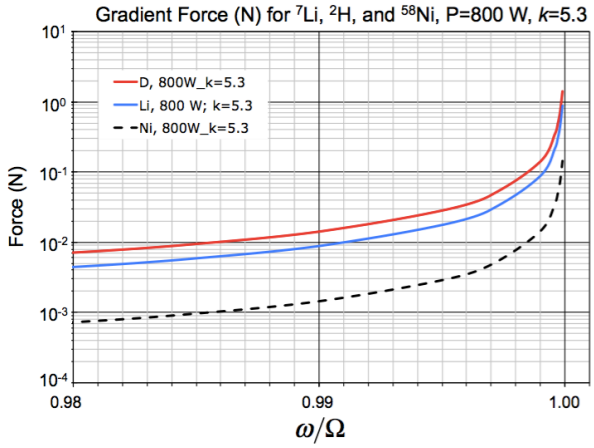

Fig. 5b Gradient forces in a model reactor operating near resonance. The input power is 800 W and geometrical amplification factor 5.3. Notice that the lower Nickel force displayed relates to the external power response. Neutron capture heating will eventually make Nickel the "hot spot, i.e. the main gradient force attractor in the reactor.

Notice that the neutron production rate is closely connected with the Gradient force, reactor temperature, and frequency near resonance (Fig. 5), the Gradient force for a given temperature being a function of frequency. During operations the net power generated inside the reactor is balanced by the radiative loss, i.e. the power emitted from the reactor surface. Equilibrium between generated and emitted power is required for continuous and stable power

production. Internal power production by neutron capture in effect leads to a chain-reaction; enhanced neutron production, further enhanced power, etc.

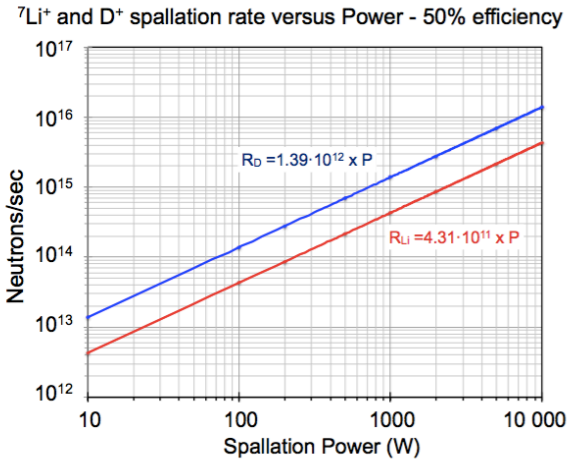

Fig. 6. Neutron production rates versus externally applied power to Lithium and Deuterium ions in the model reactor.

The internal neutron production rate is besides governed by the internal power (Fig. 6), also by the frequency of the external wave input (Fig. 5). In fact, new higher power equilibriums may be reached at preexisting power input by modulating the wave input frequency closer to resonance. This demonstrates that internal power generation becomes the main amplifying driver in the process, capable of magnifying the gain ratio (output power divided by input power) by a significant fraction (5-10). In theory, once having reached hot equilibrium the process may become almost self-sustained, driven by effective internal neutron spallation from wave input close to resonance.

Proof of concept - Experimental results

Up to now experimental results by Rossi and coworkers and their E-Cat reactor provide the best experimental verification of the RIToN process. We conclude, based on the Lugano E-Cat-experiment [23, 24] that experimental results comply with the combined spallation and neutron capture theory presented here. The isotopic shifts of lithium and nickel in the Lugano experiment fits well with the power input and power output. For instance ^{7}Li —>^{6}Li, and ^{58}Ni —>^{62}Ni agrees with the isotopic pre-, and post experiment composition values. The ^{62}Ni abundance after 32 days is consistent with the highest neutron capture cross-section of the stable nickel isotopes (Table 2). Moreover, the power gain ≈3.6 requires about 10 times more neutrons than theoretically possible from just external energy supply to the reactor, implying that internal energy spallation provides most of the neutrons during 32 days of operation.

Figs. 7, 8 and 9 describe simulations performed for ^{7}Li + Ni^{58}, and ^{2}H + Ni^{58} reactors driven to equilibrium power generation, assuming resonant Gradient forcing. The simulation considers the time dependence of core processes in the reactor, such as heating, fuel states, the evolution of spallation and neutron capture. The time dependence during all phases is illustrated in Figs. 7 and 9. During the first transition phase, essentially all power goes to partial state changes of ^{7}Li, from solid to gas, to plasma (percentage of ^{7}Li-ions up to a few percent in the reactor chamber). Resonant Gradient force acceleration of ^{7}Li-ions is assumed in the simulation. Gradient force spallation picks up rather quickly, and after a few minutes the reactor power (red), and excess power (blue) responsible for internal spallation, supersedes the nominal power input defined by the ratio between power from neutron capture and the spallation power (here 1.34).

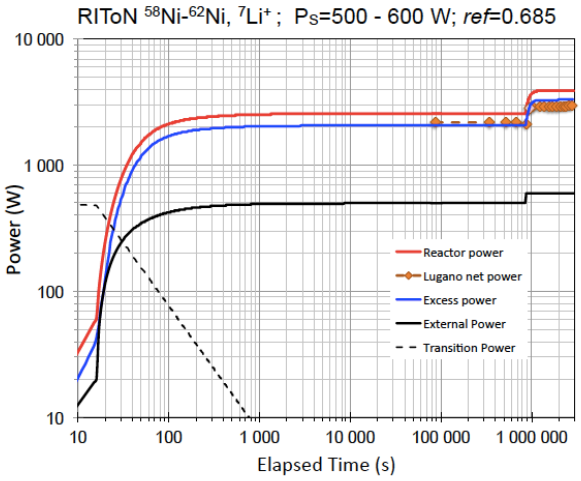

Fig. 7 Simulation of the "Lugano E-Cat" [23, 24], using comparable model input power values. Red diamonds mark the net E-Cat power [23]. Black curve marks the initial 500 W input power, increasing up to 600 W after about 11 days. Dashed curve marks the initial transition phase, were essentially all power goes to partial state changes of ^{7}Li, from solid to gas, to plasma. Notice that the 100 W increase in the simulation leads to 1400 W increase of the core power, a power amplification by a factor of 14. The latter illustrates the non-linear behavior of the system. Red curve represents the reactor core power, blue curve the excess power enabling internal neutron spallation. "ref=0.685" is an efficiency/multiplication factor, a scalar of the internal neutron production rate.

The power versus time diagram in Fig. 7 emulates fairly well the E-Cat performance in Lugano [23], noting that the simulated values correspond to reactor core power. However, there are also differences between the E-Cat and simulation. Such differences can be attributed to the more variable and complex physical processes taking place in the E-Cat reactor. The simulation is more idealized - strictly limited to, and variable within, the physical properties and boundary conditions used. Nonetheless, the simulation is adapted to the power and temperature constraints described in the Lugano-report [23], focusing on total power production.

The general agreement between simulations and E-Cat is illustrated by besides the total power, also the non-linear power amplification following a 100 W rise of input power

after ≈$9 \cdot 10^5$ seconds (≈11 days). Table 3, summarizing the simulated and measured (E-Cat) performance at maximum input power to the reactor (600 W), also display some disagreement in gain, the latter defined as the ratio between total input plus output power and the input power. Table 3 also compares the energy production after 32 days. Notice also the comparison between the annual theoretical energy production from E-Cat and the simulation, 18 and 32 MWh respectively.

The simulated RIToN gain, reactor temperature, and neutron production in Fig. 8, demonstrate the gradual changes with time. Both the reactor gain and the reactor temperatures changes with time in a similar way as that for the Lugano experiment, albeit with slightly higher simulation values.

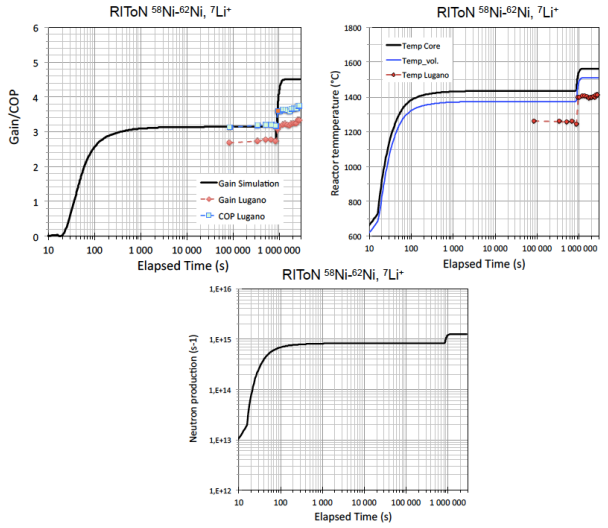

Fig. 8 Time series of physical parameters derived from the simulation and the Lugano E-Cat tests [23]. Upper two panels display a comparison between simulations and Lugano test values of gain and temperatures. The temporal evolution of simulated neutron production rates is displayed in the bottom panel.

Using the spallation rate in Fig. 8 the fuel consumption of ^{7}Li and ^{58}Ni can now be derived. Assuming an average/maximum input power of 600 W, the total number of neutrons consumed by the Lugano E-Cat after 32 days is $4.22 \cdot 10^{21}$ neutrons, corresponding to 0.049 g of Lithium. Incidentally, we note from the above number of neutrons, that the E-Cat input power [23] only sustains about 10-20% of the spallation energy required. The low external power clearly demonstrates that the excess power (Fig. 7) is the major source of neutron spallation at power equilibrium. The fuel budget for ^{58}Ni neutron capture to ^{62}Ni implies a conversion of 0.14 g ^{58}Ni.

The corresponding annual ^{7}Li and ^{58}Ni mass budget derived for continued operation of a single E-Cat-type reactor becomes 0.5 g and 1.2 g respectively, a minute fuel consumption for a device producing some 20-30 MWh per annum. Table 3 summarizes the above comparison between model simulations and the Lugano experiment.

The simulation in Fig. 9 displays the performance of a ^{2}H + ^{58}Ni reactor, noting that because of the lower spallation threshold (2.25 MeV) compared to ^{7}Li (7.2 MeV), it can operate at a much lower power input. This also leads to besides a higher power output, also a higher gain, in this case 25. Overall, the ^{2}H + ^{58}Ni reactor gives a higher performance. In fact, by combining wave input at frequencies closer to resonance with decreasing external power, (low-power mode) a new equilibrium may theoretically establish where the gain/COP may exceed 1000.

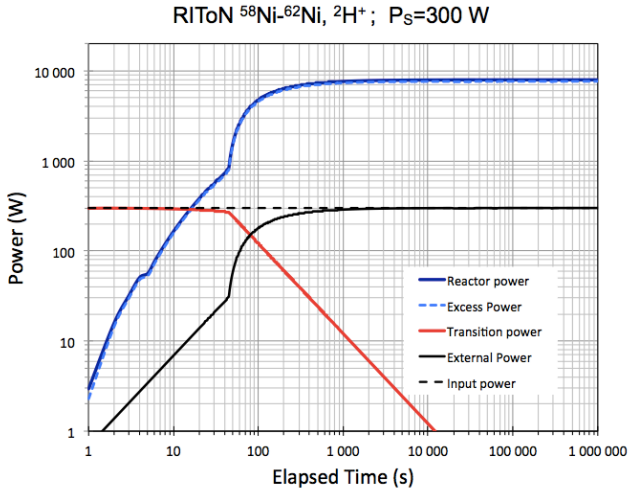

Fig. 9 same as Fig. 8, but now using Ni^{58} +^{2}H as reactor fuel, and for Grad-force 0.01 N. Compared to the Ni^{58} +^{7}Li reactor, the Ni^{58} +D reactor can be operated at lower input power (in this case 300 W), yet providing a higher gain. The gain at equilibrium is here ≈25. The above simulation of a Ni^{58} +D gives an average annual energy output/year of 69 MWh, consuming 0.7 g deuterium and 5.1 g Ni^{58}.

Conclusions

Resonant Transmutation of Nuclides, RIToN, is a process combining two isotope transmutations; resonant neutron spallation and neutron capture, the former driven by input wave energy, the latter producing energy. The process is natural, expected to occur in e.g. deuterium-enriched matter subject to high temperatures and pressure. Because the output energy is generated by neutron capture, it produces mainly low frequency radiation and benign radioactive products (e.g. via $\beta^{\pm}$-decay). This report demonstrates, theoretically and experimentally [23, 24], that nuclear energy production may be accommodated in rather small units, operating at modest temperatures (≈900-2000°C), and produce sustainable power output in the range 1 – 10 kW - at minute fuel consumption (few grams per year).

The empowering process producing neutrons, as well as maintaining the hot reactor core, is ponderomotive forcing, specifically the Gradient/Miller force. The Gradient force has three important properties: (1) The force is governed by e/m wave field gradients – i.e. gradients set

up when e/m waves penetrate into matter (solid, fluid, gas, plasma). (2) The force has a singularity with bipolar directional force shift at wave resonance, attractive below-, and repulsive above resonance. (3) The force is charge neutral, i.e. the force goes in the same direction for positive ions and electrons.

The foremost important consequence of the gradient force is that e/m radiation at frequencies below resonance attracts matter regardless of charge, the force being proportional to the e/m wave power. The hottest (most irradiative) part - the main attractor and core in a RIToN reactor - is the element subject to neutron capture (e.g. Nickel). The two most useful elements for neutron spallation are deuterium and lithium. From ^{2}H and ^{7}Li one may derive neutrons at the expense of an energy input per neutron of 2.25 MeV and 7.25 MeV respectively.

Model simulations of a ^{7}Li + ^{58}Ni reactor and experimental findings from the 32 days Lugano E-Cat test [2] are in general agreement in terms of power output, temperature, gain, and neutron production. The magnitude of the power output, delivered form a miniscule amount of fuel, demonstrates that it is a nuclear process with great potentials. Properly utilized the process has potentials of becoming a vast essentially unlimited and sustainable energy source, producing essentially no long-lived radioactive waist.

Acknowledgements

The authors are indebted to agencies (e.g. Swedish National Space Board), colleagues and friends for their support, specifically on theory and experimental investigations of ponderomotive wave forcing of space plasmas - the theoretical framework of this investigation. We are particularly thankful to Prof. Sven Kullander, who promoted a nuclear process for the "Rossi experiment" up to the bitter end (deceased 2014). The diligent work by Prof. Kullander in the Energy Committee at the Royal Academy of Sciences, and his follow-ups of the Rossi-experiment, was critical for this work.

We are thankful to Profs. Elisabeth Rachlew, and Bengt Hultqvist for valuable discussions and comments on the manuscript. Finally, one of us (RL) would like to commend a dear friend and colleague, Prof. A. Guglielmi, for the joint work that paved the way for this report.

---

[1] Lundin R., and A. Guglielmi, Ponderomotive forces in Cosmos, *Space Sci. Rev*, *.,* DOI 10.1007/s11214-006-8314-8, 2006.

[2] Lundin, Rickard and Bengt Hultqvist, *J. Geophys. Res.,* 94, 6665, 1989.

[3] Miller, M. A., *Radiophysics* (Russia), **1**, 110, 1958

[4] Allan, W, J. R. Manuel, and E. M. Poulter, Does the ponderomotive forces move mass in the magnetosphere? *Geophys. Res. Lett.*, **17**, 917, 1990.

[5] Li, X., and M. Temerin, Ponderomotive effects on ion acceleration in the auroral zone, *Geophys. Res. Lett.*, **20**, 13, 1993.

[6] Shukla, P. K., L. Stenflo, R. Bingham, and R. O. Dendy, Ponderomotive force acceleration of ions in the auroral region, *J. Geophys. Res.*, **101**, 27449, 1996.

[7] Guglielmi, A., Comment on the ponderomotive self-action of Alfvén waves, *J. Geophys. Res.*, **102**, 209, 1997.

[8] Alfvén, H., *Nature,* 150, 405, 1942.

[9] Lundqvist, S., *Phys. Rev.*, 76, 1805, 1949.

[10] Herlofson, N., *Nature*, 165, 1020, 1950.

[11] Lehnert, B., *Phys. Rev.*, 76, 1805, 1954.

[12] Buchsbaum, S. J.; Galt, J. K., *Physics of Fluids*, Vol. 4, p. 1514, 1961.

[13] Williams, G. A., 1965, *Phys. Rev.*, 139, 3a, 771-778, 1965.

[14] Galitis A., Lielausis O., Dementev S., et al., *Phys. Rev. Lett.*, 84, 4365, 2000.

[15] Booske, J.H., R-F. Cooper, S.A. Freeman, K.I. Rybakov, and V.E. Semenov, *Physics of Plasmas*, 5, 5, 1664-1670, 1998.

|16] Hamaguchi, S., R.T. Farouki, and M. Dalvie, Ponderomotive force and ion energy distributions in a rf sheath, *Phys. Rev Lett.*, 68, 1, 1992.

[17] H. L. Rowland, Anomalous absorption of electromagnetic radiation, *Physics of Fluids B: Plasma Physics* (1989-1993) 4, 3883; doi: 10.1063/1.860345, 1992.

[18] A. Singh, W. W. Destler, P. Catravas,) and J. Rodgers, Experimental study of interaction of microwaves with a nonmagnetized pulsed-plasma column, *Journal of Applied Physics*, 72, 1707; doi; 10.1063/1.351694, 1992.

[19] Sundaram, A. K., and N. Hershkowitz, Ponder-omotive force effects on temperature-gradient-driven instabilities, *Physics of Fluids* 4, 3838; doi: 10.1063/1.860340, 1992.

[20] Bruce I. Cohen and Thomas D. Rognlien, Ponderomotive and sideband coupling effects of ion-cyclotron heating on interchange stability, *Physics of Fluids* (1985) 28, 2793; doi: 10.1063/1.865239, 1985.

[21] Lundin, R. and H. Lidgren, On the attraction of matter by the ponderomotive Miller force, arXiv1005.4913L, 2010.

[22] Lidgren, H., and R. Lundin, Experimental evidence for the attraction of matter, arXiv1005; 4905L, 2010.

[23] Levi, G, E. Foshi, B. Höistad, R, Pettersson, L. Tegner, and H. Essén, Observation of abundant heat production from a reactor device and of isotopic changes in the fuel, 2014.

[24] Levi, G, E. Foshi, T. Hartmann, B. Höistad, R, Pettersson, L. Tegner, and H. Essén, Indication of anomalous heat energy production in a reactor device containing hydrogen loaded nickel powder. ArXiv 1305 3913, 2014.

Table 1. Energy budget for Li^7 neutron spallation and neutron capture by heavier isotopes, from ^{40}Ca to ^{74}Se.

Isotope	Abundance %	p	n	Binding Energy (MeV)	Neutron capture σ (b)	ΔE (MeV)	No. of neutrons rel./capt.	Lithium spallation Input (MeV)	Output (MeV)	Gain ratio
H	0.015	1	0	0		-2.245	1			
2H	99.985	1	1	2.245		0				
6Li	7.6	3	3	31.994		-7.25	1			
Li 7	92.4	3	4	39.244		0				
40Ca	96.9	20	20	342.051	0.41	0				
42Ca	0.65	20	22	361.895	0.39	19.84	2	14.50	5.34	1.37
43Ca	0.14	20	23	369.828	6.20	27.78	3	21.75	6.03	1.28
44Ca	0.14	20	24	380.960	0.88	38.91	4	29.00	9.91	1.34
58Ni	68.1	28	30	506.460	4.37	0				
60Ni	26.2	28	32	526.850	2.50	20.39	2	14.50	5.89	1.41
61Ni	1.1	28	33	534.660	2.10	28.20	3	21.75	6.45	1.30
62Ni	3.6	28	34	561.750	14.90	38.80	4	29.00	9.80	1.34
64Ni	0.9	28	36	561.754	1.64	55.29	6	43.50	11.79	1.27
65Ni		28	37	567.852	22.40	61.39	7	50.75	10.64	1.21
65Cu		29	36	569.207		62.75		50.75	12.00	1.24
46Ti	8.25	22	24	398.194	0.59	0				
48Ti	73.7	22	25	418.698	8.30	20.50	2	14.50	6.00	1.41
50Ti	5.2	22	26	437.780	0.18	39.59	4	29.00	10.59	1.37
52Cr	83.8	24	28	456.345	0.86	0				
54Cr	2.4	24	30	474.003	0.41	17.66	2	14.50	3.16	1.22
64Zn	49.2	30	34	559.093	0.79	0				
66Zn	18.5	30	36	579.113	1.00	20.02	2	14.50	5.52	1.38
70Ge	20.6	32	38	610.517	3.10	0				
74Ge	36.5	32	42	645.664	0.52	35.15	4	29.00	6.15	1.21
74Se	0.9	34	40	642.890	52.2	0				
76Se	9.4	34	42	662.070	84.8	19.18	2	14.50	4.68	1.32
78Se	23.8	34	44	679.988	0.43	37.10	4	29.00	8.10	1.28
80Se	49.6	34	46	696.865	0.58	53.98	6	43.50	10.48	1.24

Table 2. Energy budget for thermal neutron spallation and thermal neutron capture by Ni^{58}, comparison between Li^{7} and Deuterium. Notice the high thermal neutron capture of Ni^{65}. Following the capture of 7 neutrons the unstable Ni^{65} converts to Cu^{65} via electron capture.

								Lithium spallation			**Deuterium spallation**		
	Abundancy			Binding Energy	Neutron capture	ΔE	No. neutr.	Input	Output	Gain	Input	Output	Gain
Isotope	%	p	n	(MeV)	σ (b)	(MeV)	capt.	(MeV)	(MeV)	ratio	(MeV)	(MeV)	ratio
H	99.985	1	0	0		-2.245	1						
2H	0.015	1	1	2.245		0							
6Li	7.6	3	3	31.994		-7.25	1						
7Li	92.4	3	4	39.244		0							
58Ni	68.1	28	30	506.460	4.37	0							
59Ni	-	28	31	515.435	77.7	8,994	1	7.25	1.744	1.24	2.25	6.75	4.00
60Ni	26.2	28	32	526.850	2.50	20.39	2	14.50	5.89	1.41	4.49	15.90	4.54
61Ni	1.1	28	33	534.660	2.10	28.20	3	21.75	6.45	1.30	6.74	21.47	4.19
62Ni	3.6	28	34	545.258	14.90	38.80	4	29.00	9.80	1.34	8.98	29.82	4.32
63Ni	-	28	35	552.100	24.40	45.64	5	36.25	9.39	1.26	11.23	34.42	4.07
63Cu	*69.5*	*29*	*34*	*55.,376*	*4.5*	*44.92*	*5*	*36.25*	*8.67*	*1.24*	*11.23*	*33.69*	*4.00*
64Ni	0.9	28	36	561.754	1.64	55.29	6	43.50	11.79	1.27	13.47	41.82	4.10
65Ni	-	28	37	567.852	22.40	61.39	7	50.75	10.64	1.21	15.72	45.68	3.91
65Cu	*30.9*	*29*	*36*	*569.207*		*62.75*	*7*	*50.75*	*12.00*	*1.24*	*15.72*	*62.75*	*3.99*

Table 3. Comparison between the power budget and gain factor for the model reactor and the CCat Lugano experiment [2]. Included are also estimates of the annual energy production.

	Model reactor	E-Cat Lugano
Reactor power (W)	3800	2113
Average input power (W)	600	599
Gain factor*	4.5	3.7
Sum Energy, 32 days (J)*	$1.1 \cdot 10^{10}$	$5.8 \cdot 10^{9}$
Sum Energy, 1 year (MWh)*	33	18

*Excluding system losses

Table 4. Simulated model values for the Spallation rate and fuel (^{7}Li and ^{58}Ni) consumption derived from the simulations based on the Lugano experiment (Fig. 8) at maximum power consumption. Notice the low annual fuel consumption (≈1 – 4 grams).

	Model	
^{7}Li spallation rate	$1.50 \cdot 10^{15}$	neutrons/s
Sum ^{7}Li spallations, 32 days	$4.2 \cdot 10^{21}$	neutrons
1 g ^{7}Li corresponds to	$8.56 \cdot 10^{22}$	neutrons
Sum ^{7}Li mass, 32 days	0.049	g
$\sum^{58}Ni$ -^{62}Ni captures, 32 days	$1.4 \cdot 10^{21}$	captures
$\sum$ ^{58}Ni mass, 32 days	0.14	g
$\sum$ ^{7}Li mass, 1 year	0.55	g
$\sum$ ^{58}Ni mass, 1 year	1.2	g

Institutet för rymdfysik

Swedish Institute of Space Physics

Swedish Institute of Space Physics
Box 812, SE- 981 28 Kiruna, SWEDEN
tel. +46-980-790 00, fax +46-980-790 50, e-post: irf@irf.se

www.irf.se